AFOSR SCIENTIFIC REPORT NO. 65-0313

" A TRIAXIAL EXPERIMENT ON YIELD CONDITION IN PLASTICITY"

by

L. W. Hu, J. Markowitz, T. A. Bartush

Grant No.: AFOSR 127-64

AIR FORCE OFFICE OF SCIENTIFIC RESEARCH
Directorate of Engineering Sciences
Washington, D.C. 20333

The Pennsylvania State University
Department of Engineering Mechanics
University Park, Pennsylvania

January 1965

LIMITATIONS IN REPRODUCTION QUALITY OF TECHNICAL ABSTRACT BULLETIN DOCUMENTS, DEFENSE DOCUMENTATION CENTER (DDC)

AD 614574

- [ ] 1. AVAILABLE ONLY FOR REFERENCE USE AT DDC FIELD SERVICES. COPY IS NOT AVAILABLE FOR PUBLIC SALE.
- [x] 2. AVAILABLE COPY WILL NOT PERMIT FULLY LEGIBLE REPRODUCTION. REPRODUCTION WILL BE MADE IF REQUESTED BY USERS OF DDC.
  - [x] A. COPY IS AVAILABLE FOR PUBLIC SALE.
  - [ ] B. COPY IS NOT AVAILABLE FOR PUBLIC SALE.
- [ ] 3. LIMITED NUMBER OF COPIES CONTAINING COLOR OTHER THAN BLACK AND WHITE ARE AVAILABLE UNTIL STOCK IS EXHAUSTED. REPRODUCTIONS WILL BE MADE IN BLACK AND WHITE ONLY.

TSL-121-2/64

DATE PROCESSED: 5-11-65

PROCESSOR: D. Lee

Abstract

A triaxial stress experiment was developed for the determination of the intersections of the initial and subsequent yield surfaces with a hydrostatic stress-principal stress plane. Results of an experiment on Nittany Brass No. 2 of the soft grade were reported. Information so obtained makes it possible for one to see the yield condition in the sense of a three dimensional surface rather than a two dimensional curve as observed in conventional biaxial stress tests.

A Triaxial Stress Experiment on Yield Condition in Plasticity

by

L. W. Hu*, J. Markowitz* and T. A. Bartush*

1. Introduction

A yield condition specifies the state of stress under which yielding or additional plastic deformation may occur in a strained body. Such a yield condition can be represented graphically as a so-called yield surface in the stress space as shown in Fig. 1. In the last few decades, numerous experimental investigations have been made to determine the initial yield surface as well as the effect of plastic deformation on the subsequent yield surfaces by means of biaxial stress experiments. Evidently these experiments have been capable only of studying the shape and behavior of the intersection of the yield surface with a two-dimensional stress plane. For example, Fig. 2 shows the effect of tensile plastic deformation on the yield condition in a plane of two principal stresses as observed by biaxial tension-tension tests (1)**. Figure 3 shows the effects of shear strain on the yield condition in the tension-shear plane as observed by biaxial tension-torsion tests (2). Since the yield surface is three dimensional in nature, experimental results so obtained do not provide sufficient information

* Department of Engineering Mechanics, The Pennsylvania State University, University Park, Pennsylvania.

** Numbers in brackets refer to the References at the end of the paper.

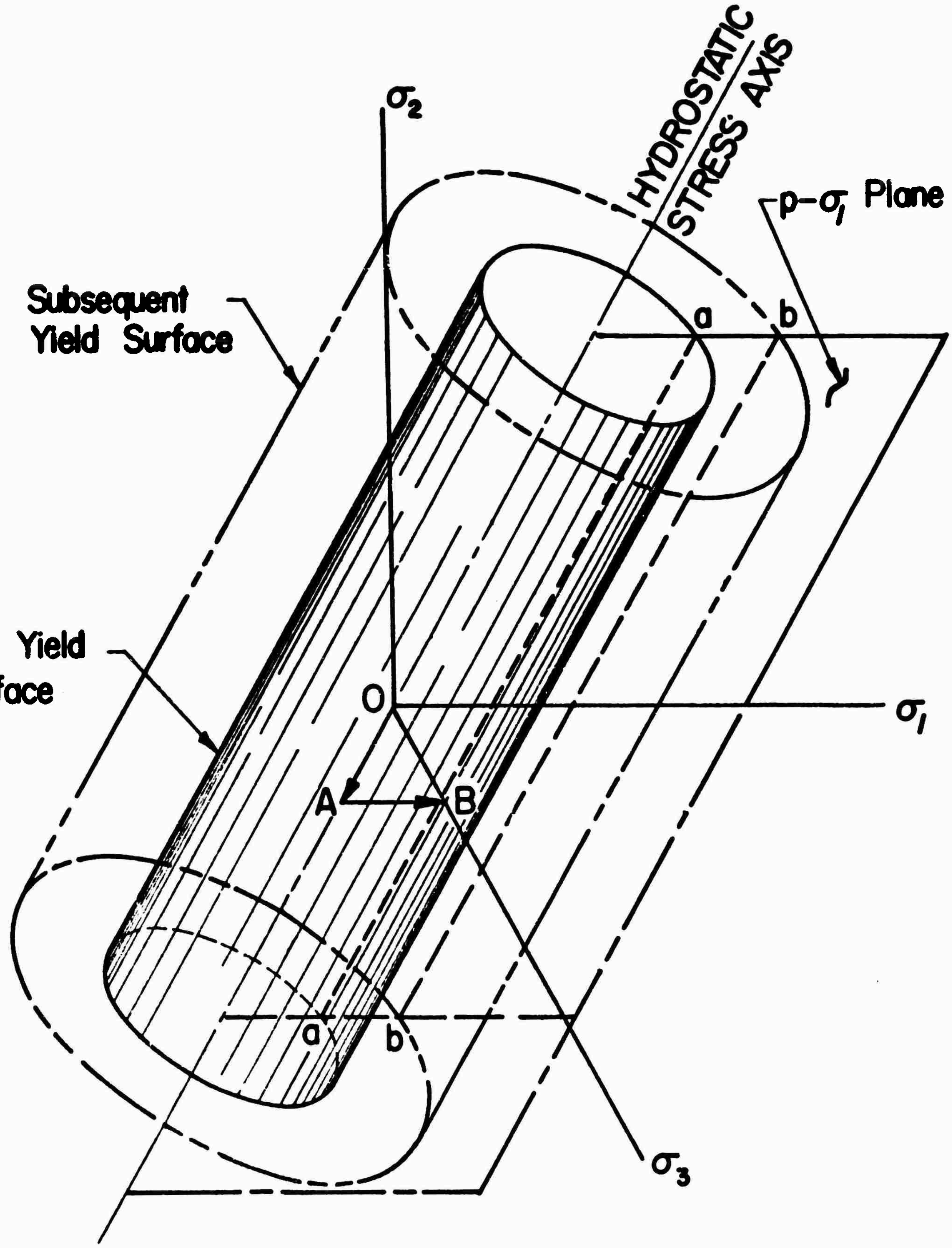

FIG. 1 DETERMINATION OF INITIAL YIELD SURFACE

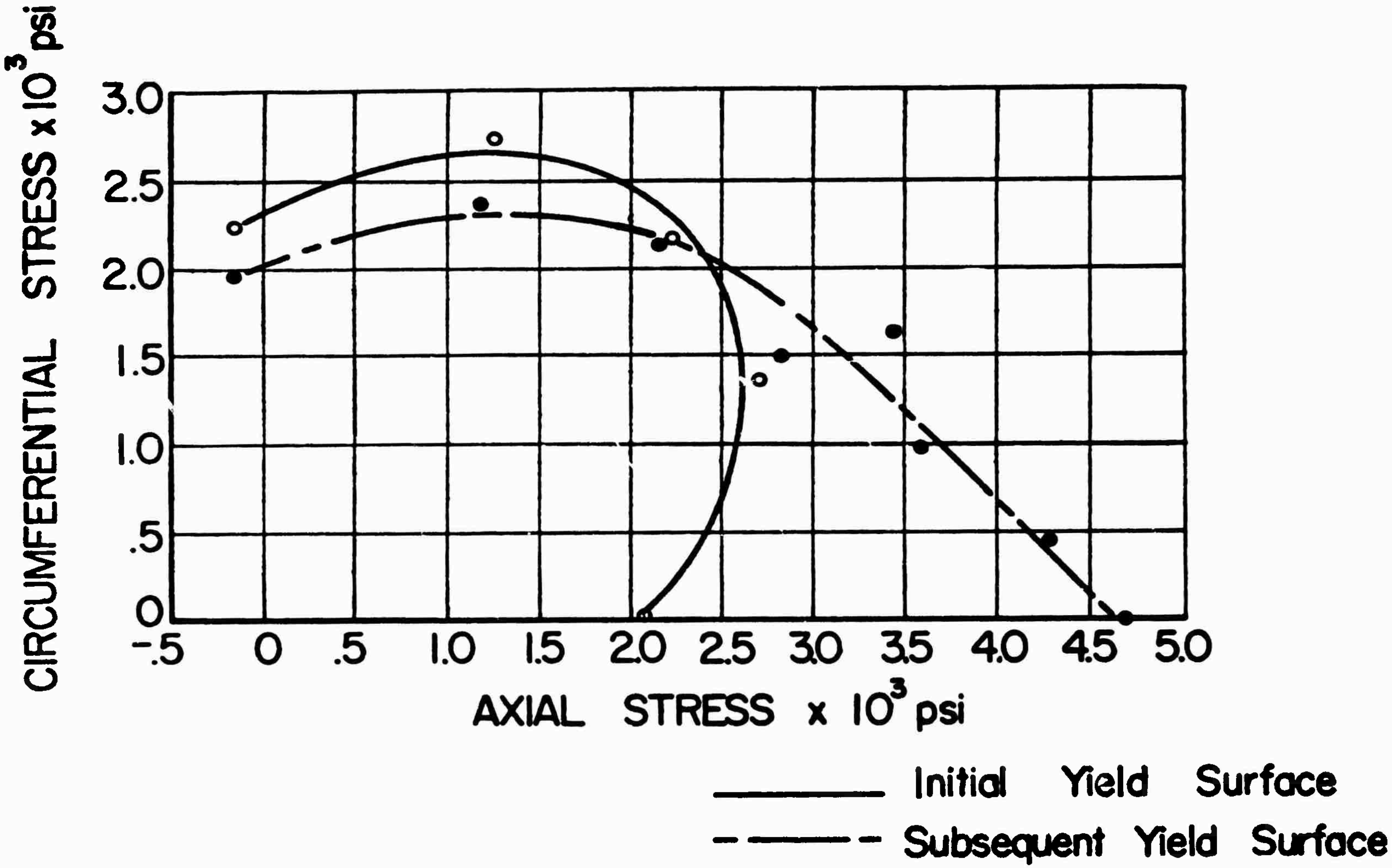

FIG. 2 BIAXIAL TENSION-TENSION EXPERIMENT

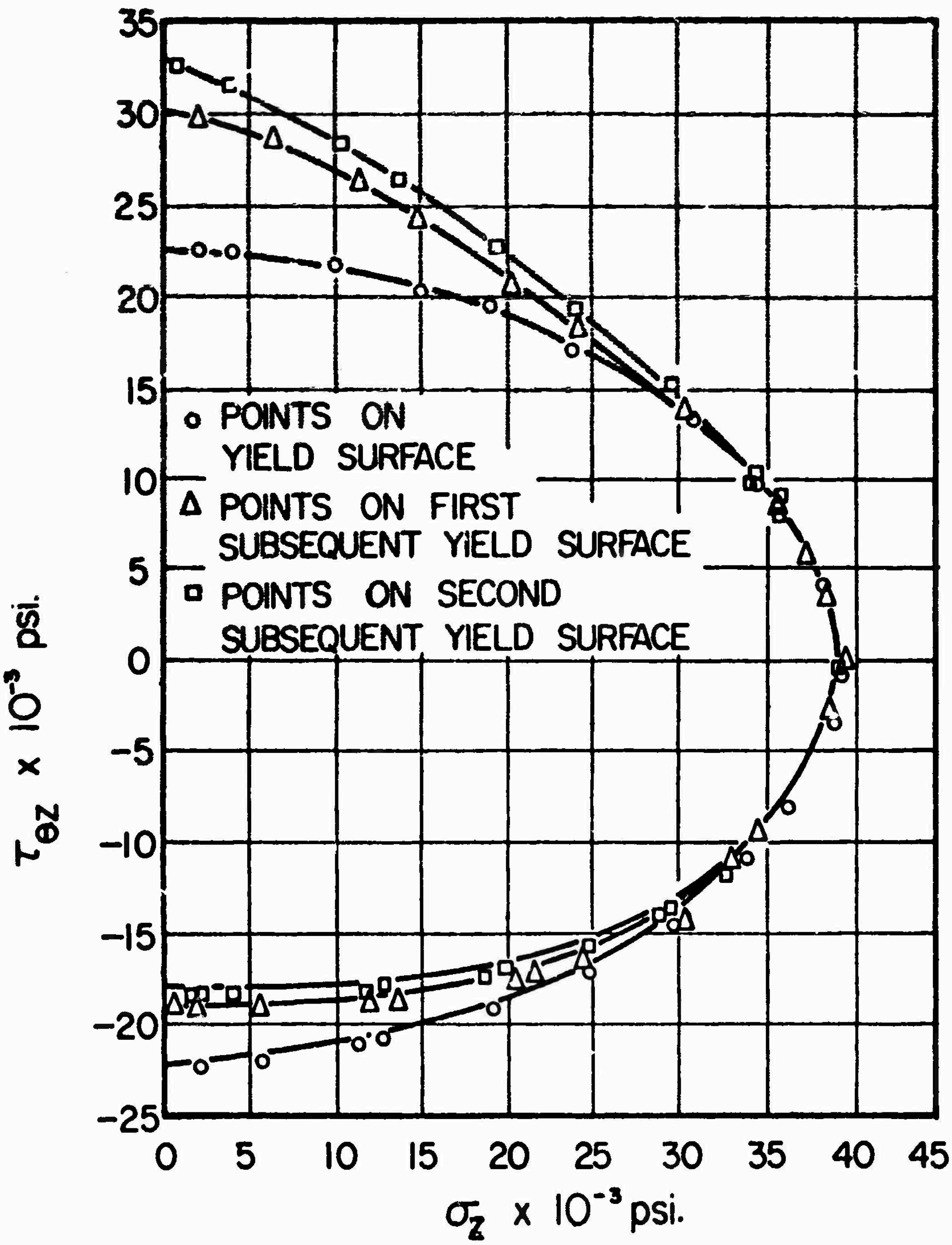

FIG. 3 BIAXIAL TENSION-TORSION EXPERIMENT

to describe the shape of the initial and subsequent yield surfaces. In other words, the biaxial stress experiments are not adequate for the determination of the yield conditions and strain-hardening of metals.

The present investigation presents a triaxial stress experiment designed to study the effect of plastic deformation on the subsequent yield surfaces in three dimensional stress space. Such a method is capable of determining the intersections of the yield surface with the hydrostatic stress-axial stress plane, say p - σ_1 plane as shown in Fig. 1. It is believed that experiments of this type may yield a complete understanding of the yielding and strain-hardening of metals under combined stresses.

2. Yield Conditions in Plasticity

A stress state at a material point may be decomposed into a hydrostatic stress component and a deviatoric stress component. Yielding or plastic flow may occur at this material point when a specific function f of stress deviators reaches a critical value. In turn, the function f and the magnitude of this critical value may be influenced by the intensity of the hydrostatic stress component (3). Graphically the yield condition can be represented by a cylindrical surface which encloses the hydrostatic stress axis passing through the origin and having direction cosines $(1/\sqrt{3},\ 1/\sqrt{3},\ 1/\sqrt{3})$ in the principal stress space. If the plastic flow of metals is not affected by the hydrostatic stresses, the generator of the yield surface becomes a straight line parallel to the hydrostatic stress axis as shown in Fig. 1. Then the function of stress deviators will determine the shape of the cross section of this surface.

For materials with strain-hardening, the plastic deformation will cause changes in the yield condition. Namely, the shape and the dimensions of the subsequent yield surfaces are affected by the strain history of the plastically deformed body. The basic modes of changes of the yield surfaces have been discussed by Hu and Marin (4) and Prager (5) but the discussion has been limited to the two dimensional stress plane. In order to obtain a complete and correct understanding of the behavior of the initial and subsequent yield surfaces for strain-hardening materials, it is necessary to describe the changes of yield surfaces in the three dimensional stress space.

From the consideration of the geometry of the yield surface, the basic modes of expansion of the yield surface may be classified as follows:

a. Isotropic expansion

b. Translation in the direction of a stress vector

c. Translation in the direction of a stress rate vector

d. Translation in the direction of a strain rate vector

e. Rotation about the axis of the yield surface

f. Rotation about a line perpendicular to the axis of the yield surface

g. Formation of local bulge.

The initial yield surface may expand into a subsequent yield surface by means of one or a combination of these basic modes of expansion. In other words, the knowledge of the existence and correctness of these basic modes of expansion is essential to the formulation of plastic stress strain relations for metals with strain-hardening.

3. Specimens and Testing Machine

Sixty tension specimens of the dimensions shown in Fig. 4 were made of the Nittany No. 2 brass of the soft grade. The material was supplied by the Titan Metal Manufacturing Company of the Cerro Corporation in the form of 10-feet bar stock 3/4 inch in diameter. Specimens were tested in the as-received condition. The nominal chemical composition is given as follows: copper 61.5%; lead 3.25%; iron, nickel and tin each less than 0.10%; and zinc, the balance.

To determine the tensile properties of the material, control tests were conducted in a 12,000 lb. X-Y Electromatic Universal Testing Machine manufactured by Tinius Olson Testing Machine Company. Cross-head speeds of 0.2, 2.0 and 20 in./min. were used and no strain rate effect was observed. However, it was found that the mechanical properties showed slight variations from bar to bar. Consequently, all specimens in the following experiments were subjected to a prestress of 18,300 psi. which is 5% above the average proportional limit of the material.

The triaxial stress testing machine used in this investigation is the one reported in Reference (6) with some modifications in the pressure generating unit and the recording system. Only these modifications are to be described in the following paragraphs.

The hydrostatic pressure in the testing section of the machine was generated by a Harwood Pressure System with a SA14-8-1.250-200K single acting intensifier. The pressure fluid used was Sovasol supplied by the Mobil Oil Company.

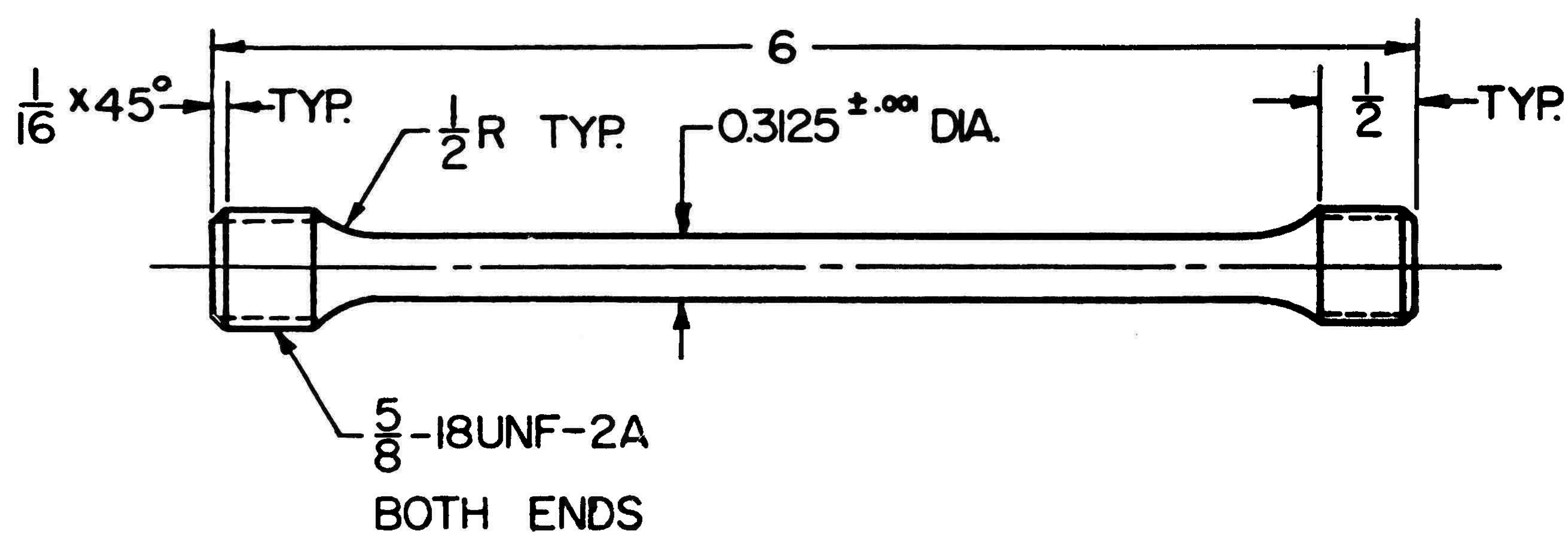

FIG. 4 TENSION SPECIMEN

For recording, a two-channel strain gage recorder made by the Sanborn Company was used. The unit consisted of two Strain Gage Amplifiers of Model 64-500BDS, a Detector Shunt of Model 60-2100, a Control Panel of Model 60-1600 and a Twin-Viso Recorder of Model 60-1300B. During the experiment, the intensity of the hydrostatic pressure was recorded by one channel and the load on a piston was recorded by the other. The load in the specimen under hydrostatic pressure was evaluated from the recorded load-time curve by a procedure similar to the one described in Reference (7).

4. Experimental Procedures

Three series of tests were conducted to study the effect of tensile plastic deformation on the yield surface. The first series was to determine the shape of the initial yield surface of the material tested. The second and third series were to determine the changes in the shape of the subsequent yield surface after the material was prestressed in tension to 31,390 psi. and 39,240 psi. respectively.

In the first series of tests, after the specimen was placed in the triaxial stress testing machine, hydrostatic pressure of the prescribed intensity p was applied. Namely, the specimen was first subjected to a stress state of three equal principal stresses $\sigma_1 = \sigma_2 = \sigma_3 = -p$. Then an axial tension was applied to the specimen in addition in the manner described in Reference (7). Then the state of stress in the specimen became

$$\sigma_1 = \sigma - p$$

$$\sigma_2 = \sigma_3 = -p$$

The yielding of the specimen was observed on a load-time curve recorded by the Sanborn Recorder. The yield stress was computed on the basis of the load P at yield evaluated from the load-time curve by the procedure used in Reference (7). The strain rate at yielding was about 0.01 in./in./sec. as estimated from the load-time curve. After yielding, the load and the hydrostatic pressure were released.

In the second and the third series of tests, the specimens were prestressed in tension at atmospheric pressure first. Then the yield stresses under various hydrostatic pressures were determined in a manner similar to the first series of tests. A set of load-time curves from the third series of tests is shown in Fig. 5. It should be noted that the gain of the Strain Gage Amplifier was adjusted to suit the pressure level at which a test was conducted. All tests in these two series were conducted within one hour after the specimens were prestressed. The purpose of such an action was to minimize any possible age-hardening effect on the properties of prestressed specimens.

5. Experimental Results and Discussion

The loading program employed in the first series of tests was the gradual application of a prescribed hydrostatic pressure to the specimen as represented by line O-A in Fig. 1. Then axial tension applied as shown by line A-B. Yielding will occur when the line AB reaches the initial yield surface at point B. In other words, a point B on the initial yield surface can be located by following the loading program O-A-B and observing the magnitude of the axial load at the incipience of yielding. This loading program O-A-B obviously lies in the plane

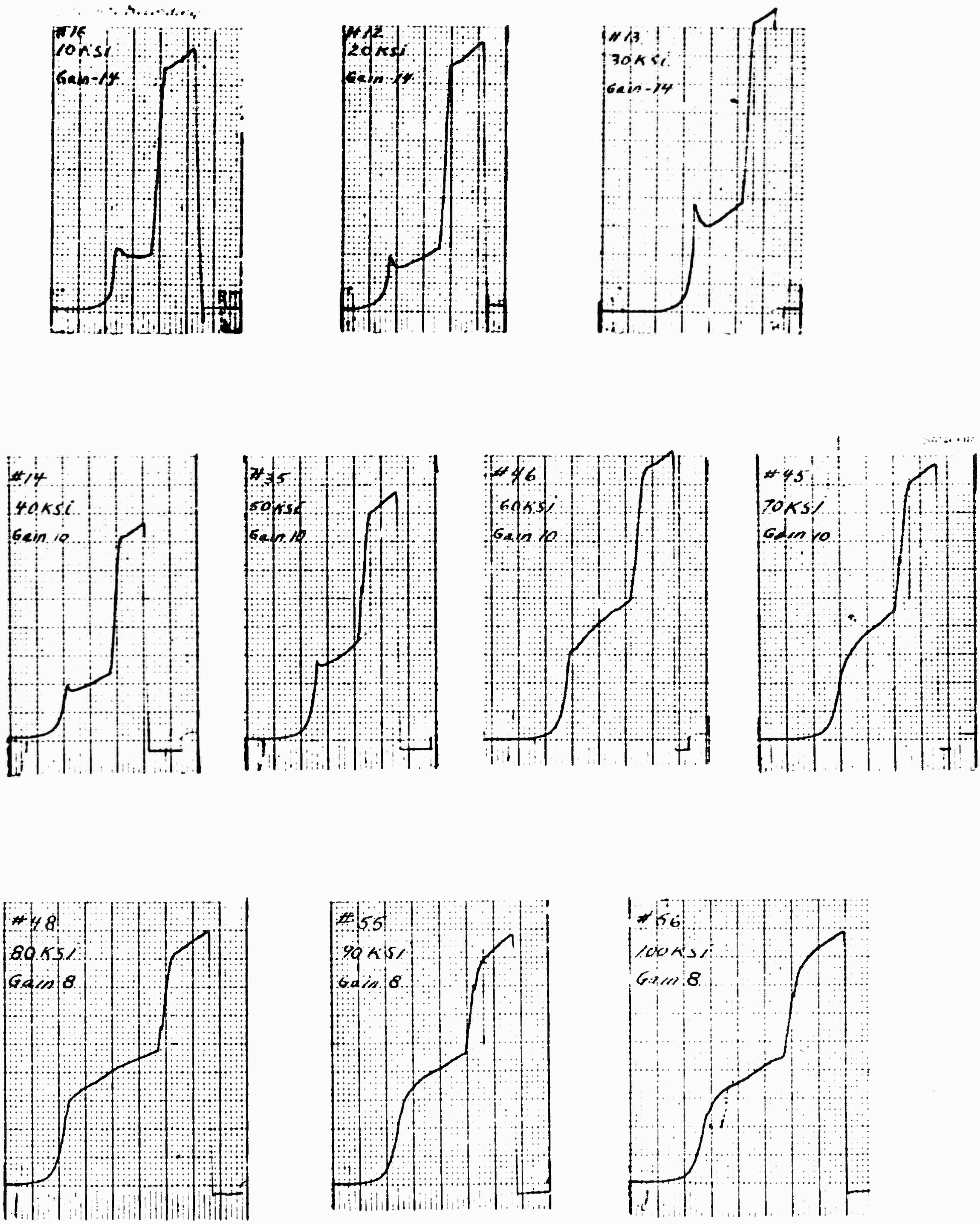

FIG. 5 TYPICAL LOAD-TIME CURVES - SERIES III

which contains the hydrostatic stress axis and a principal stress axis, say σ_1-axis. This plane hereafter is referred to as the $p - \sigma_1$ plane. By subjecting specimens to this loading program at various hydrostatic pressures, a number of points on the intersection of the initial yield surface and the $p - \sigma_1$ plane can be determined.

Now, consider the specimen being first plastically deformed by axial tension at atmospheric pressure as shown by the loading path O-A-B-A-O in Fig. 6. Point A represents the initial yield point of the specimen, and A-B represents the extent of stressing into plastic region. As a result of this loading, the yield surface will expand outwards to contain the point B and subsequently becomes a new yield surface. Since unloading is an elastic process, the removal of the tensile load along the path B-A-O should not cause any change in the new yield surface. Then the intersection of the new or subsequent yield surface with the $p - \sigma_1$ plane can be determined by the loading program employed in the first series of tests. Therefore, in the second and third series of tests, the loading program O-A-B-A-O-C-E was used to determine the intersections of the subsequent yield surfaces with the $p - \sigma_1$ plane.

The results of the three series of triaxial stress experiments on Nittany No. 2 brass are given in Table 1. Figure 7 shows the yield stresses at various pressures as observed in the three series of experiments described. The intersections of the initial and subsequent yield surfaces with the $p - \sigma_1$ plane so determined are shown in Fig. 8. Significantly, instead of being straight lines parallel to the hydrostatic stress axis, both curves II and III show that the tensile yield stress of the specimens prestressed plastically in tension

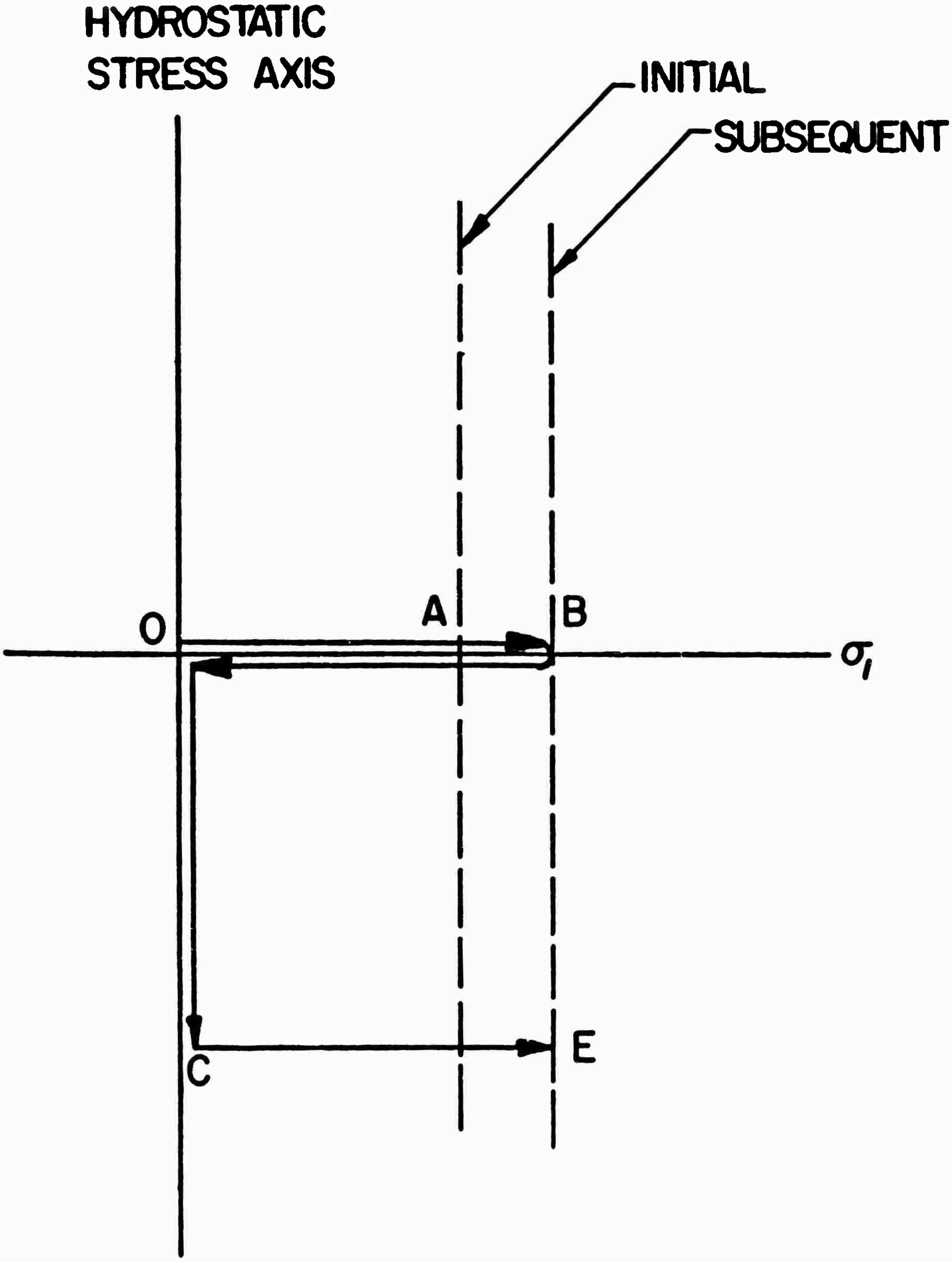

FIG. 6 LOADING PROGRAM FOR TESTS OF SERIES II & III

Series I Prestress - 18,310 psi					Series II Prestress - 31,380 psi					Series III Prestress 39,240 psi				
Spec. No.	Test Pressure (psi)	Yield Stress (psi)	Average Yield Stress (psi)	% Change	Spec. No.	Test Pressure (psi)	Yield Stress (psi)	Average Yield Stress (psi)	% Change	Spec. No.	Test Pressure (psi)	Yield Stress (psi)	Average Yield Stress (psi)	% Change
55	10,930	17,790	18,450	+0.76	23	10,930	31,260	30,610	-2.48	11	10,930	38,190	38,460	-1.98
56	10,930	19,100			19	10,930	29,950			16	10,930	38,720		
47	21,350	17,660	18,050	-1.42	20	21,350	30,350	29,760	-5.19	12	21,350	37,280	38,000	-3.16
50	21,350	18,440			24	21,350	29,170			17	21,350	38,720		
49	31,540	17,270	17,210	-6.00	21	31,540	28,650	28,980	-7.68	13	31,540	37,670	36,950	-5.83
46	31,540	17,140			25	31,540	29,300			18	31,540	36,230		
48	41,290	15,960	16,220	-11.41	26	41,290	28,120	28,790	-9.28	14	41,290	38,460	36,960	-5.81
45	41,290	16,480			22	41,290	29,820			32	41,290	35,450		
36	50,850	16,480	15,830	-13.54	29	49,900	26,420	26,420	-15.83	15	50,850	35,320	34,860	-11.16
44	50,850	15,170								35	50,850	34,400		
35	60,480	15,960	16,620	-9.23	28	50,850	27,080	27,870	-11.21	36	60,480	35,060	34,300	-11.31
32	60,480	17,270			27	50,850	28,650			46	60,480	34,530		
34	70,110	16,350	15,960	-21.83	49	60,480	27,210	27,150	-13.50	45	70,110	33,090	33,420	-14.83
31	70,110	15,570			39	60,480	27,080			47	70,110	33,750		
33	79,510	16,610	16,680	-8.90	47	70,110	24,070	25,510	-18.73	48	79,510	32,700	33,360	-14.98
30	79,510	16,740			41	70,110	26,950			49	79,510	34,010		
52	89,040	16,870	16,740	-8.57	50	79,510	25,110	24,330	-21.85	50	89,040	32,310	31,260	-20.33
51	89,040	16,610			42	79,510	23,940			55	89,040	30,210		
54	97,970	17,270	16,750	-8.52	57	89,040	25,250	23,550	-25.00	56	47,970	30,350	30,350	-22.65
53	97,970	16,220			58	89,040	21,840							
					59	97,970	23,540	23,220	-26.03					
					60	97,970	22,890							

TABLE I Experimental Results

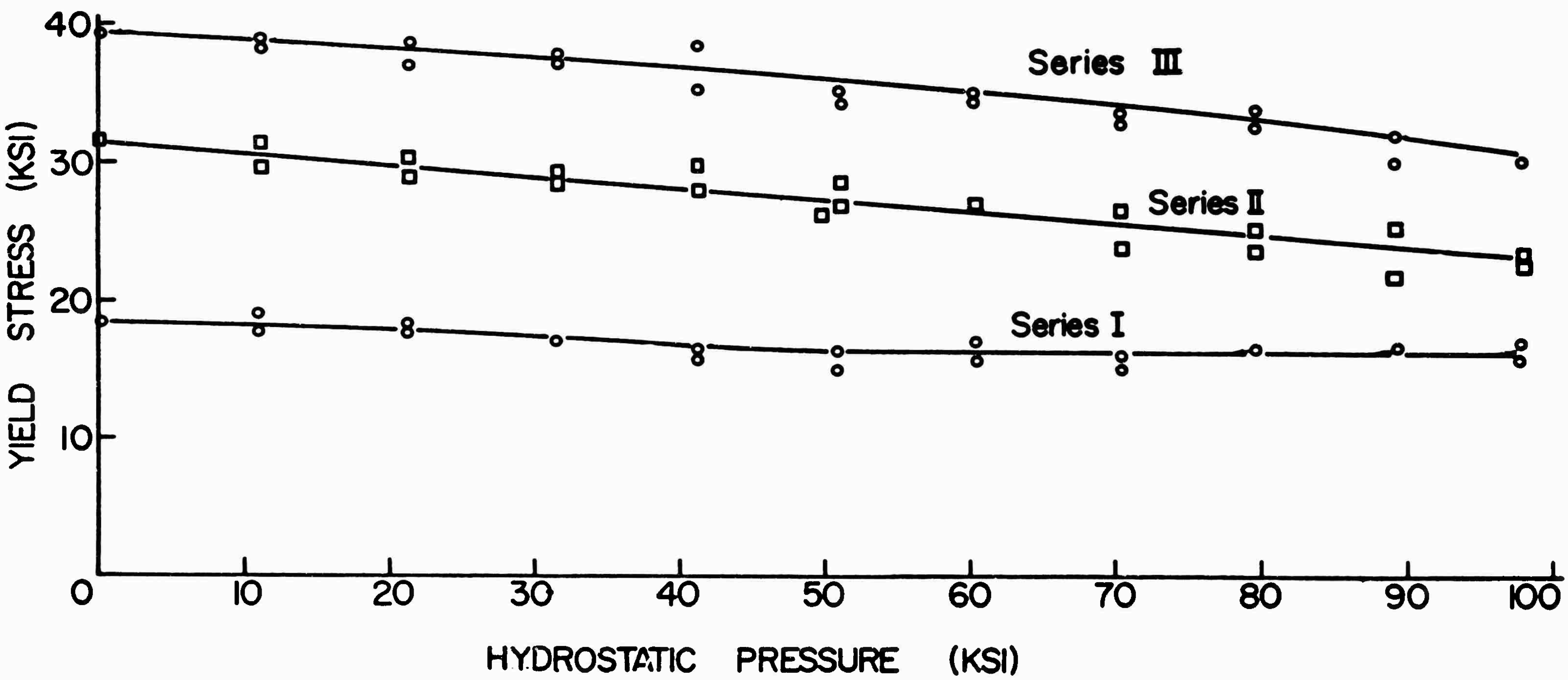

FIG. 7 VARIATION OF YIELD STRESS WITH HYDROSTATIC PRESSURE

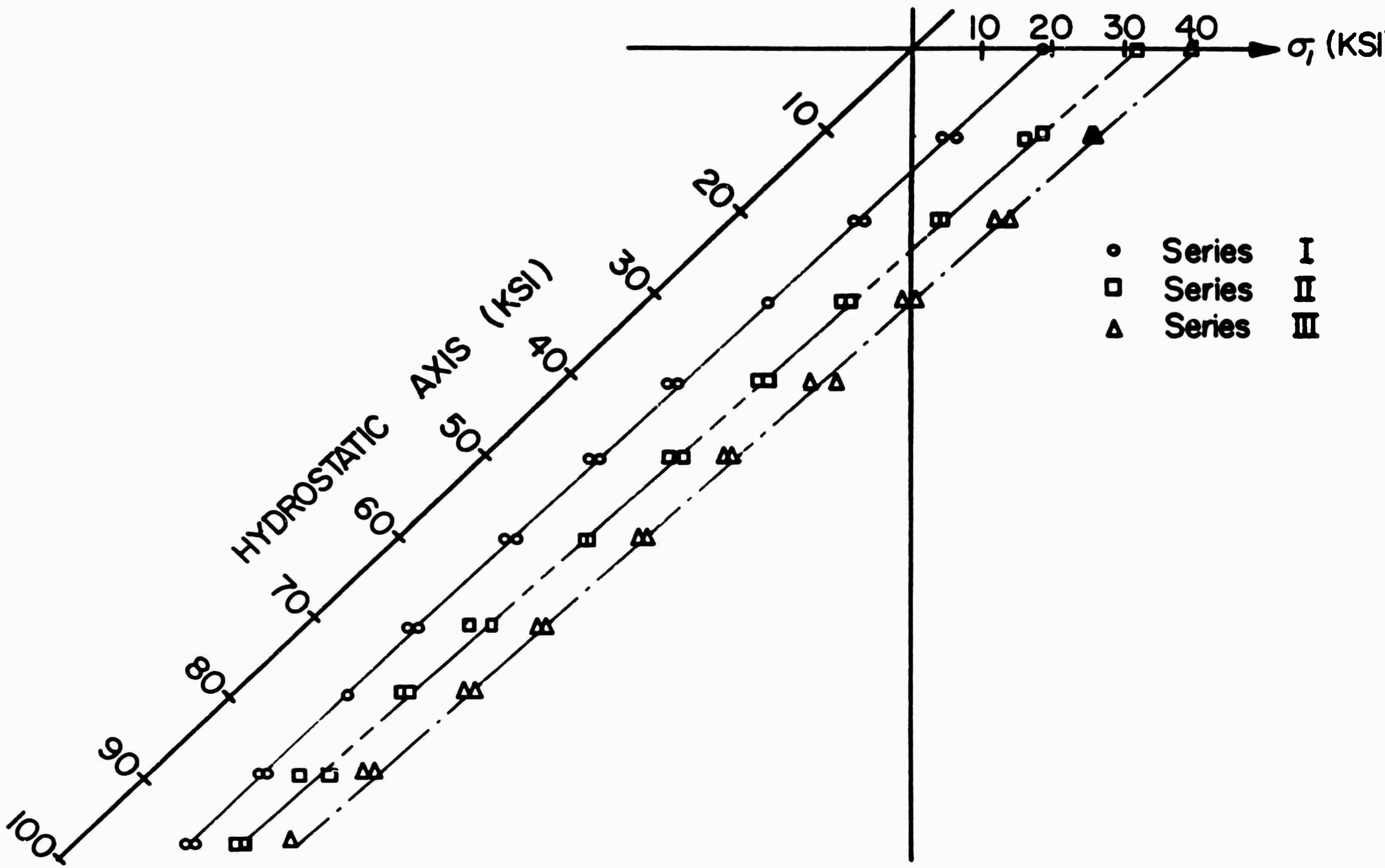

FIG. 8 INTERSECTION OF INITIAL AND SUBSEQUENT YIELD SURFACE WITH $p-\sigma_1$ PLANE

decreases when the intensity of the superimposed hydrostatic pressure increases. The percentage reduction in yield stress at each pressure level for Series II and III is shown in Table 1. This fact leads to the following conclusions for the material tested.

First, if the concept of isotropic strain hardening is valid, the intersections of the subsequent yield surfaces with the $p - \sigma_1$ plane should be parallel to the intersection of the initial yield surface with the $p - \sigma_1$ plane, but the experimental results definitely indicate otherwise. It may be concluded that the experimental results invalidate the concept of isotropic strain-hardening, i.e., isotropic expansion of yield surface. The same conclusion has been arrived at previously by observations of biaxial stress experiments. In other words, the plastic stress strain relation of the form

$$\phi_1 (J_2' , J_3') = \psi_1(\bar{\epsilon}_p)$$

or

$$\phi_2 (J_2' , J_3') = \int d\bar{\epsilon}_p$$

is not applicable. J_2' and J_3' are the second and third invariants of stress deviators, and $\bar{\epsilon}_p$ is the generalized plastic strain.

Second, the experimental results cannot be explained by the translation of yield surface alone as postulated by the kinematic theory of strain hardening (5), for a pure translation of the yield surface would have the intersections of the initial and subsequent yield surfaces with the $p - \sigma_1$ plane parallel to each other.

Third, it appears that the formation of a local bulge on the initial yield surface as shown in Fig. 9 can explain both the experimental

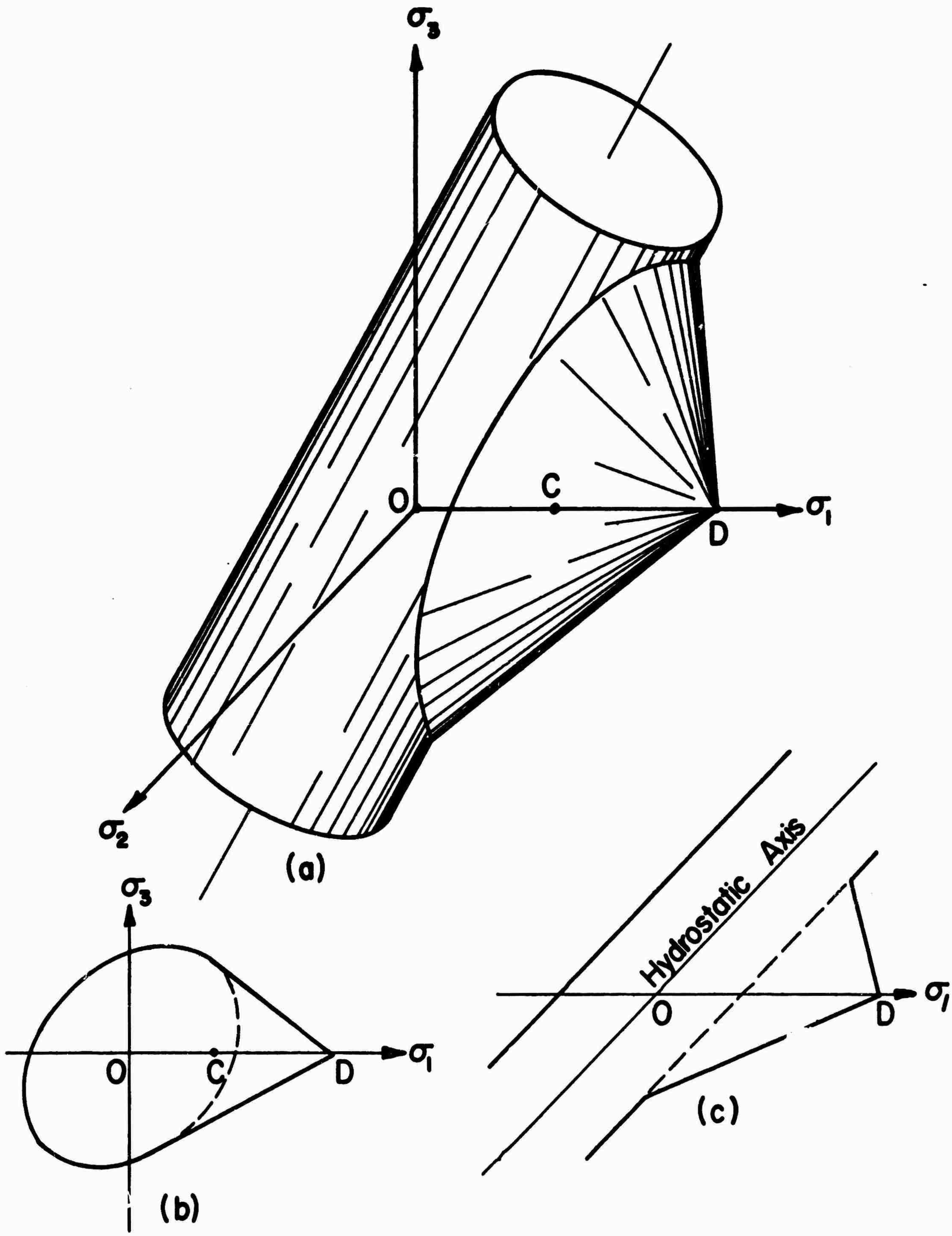

FIG. 9 BULGE FORMATION DUE TO LOADING PATH OCD

results obtained and the evidence of the yield corner formation observed in biaxial stress experiments previously (1,2). In such a mode of expansion of the yield surface, the intersections of the yield surface with a biaxial stress plane and the $p - \sigma_1$ plane have the characteristics observed in the biaxial stress and triaxial stress experiments respectively (Fig. 9). Certainly, the shape of the subsequent yield surface may be a combination of the formation of local bulge and other modes of expansion. Further experimental information is needed for clarification.

6. Acknowledgment

The investigation presented in this paper is part of a grant on "Experimental and Analytical Studies in Theory of Plasticity with Hydrostatic Stress Effect" sponsored by the Air Force Office of Scientific Research, U. S. Air Force.

REFERENCES

1. Hu, L. W. and Bratt, J. F., "Effect of Tensile Plastic Deformation on Yield Condition," Journal of Applied Mechanics, Vol. 25, No. 3, p. 411, 1958.

2. Naghdi, P. M., Essenberg, F. and Koff, W., "An Experimental Study of Initial and Subsequent Yield Surfaces in Plasticity," Journal of Applied Mechanics, Vol. 25, pp. 201-209, 1958.

3. Hu, L. W., "Plastic Stress-Strain Relations and Hydrostatic Stress," Proceedings of Second Symposium on Naval Structural Mechanics, Pergamon Press, 1960, pp. 194-201.

4. Hu, L. W. and Marin, J., "Anisotropic Loading Functions for Combined Stresses in the Plastic Range," Journal of Applied Mechanics, Vol. 22, No. 1, 1955, pp. 77-85.

5. Prager, W., "The Theory of Plasticity: A Survey of Recent Achievements," Proc. Institution of Mechanical Engineers, Vol. 169, No. 21, 1955.

6. Hu, L. W., "Development of Triaxial Stress Testing Machine and Triaxial Stress Experiments," Proc. of the Society for Experimental Stress Analysis, Vol. 16, No. 2, pp. 27-37, 1959.

7. Hu, L. W., "Determination of the Plastic Stress Strain Relations in Tension for Nittany No. 2 Brass under Hydrostatic Pressure," Proc. 3rd U.S. National Congress of Applied Mechanics, pp. 63-65, 1958.

List of Captions

Figure 1 Determination of initial yield surface.

Figure 2 Biaxial tension-tension experiment.

Figure 3 Biaxial tension-torsion experiment.

Figure 4 Tension specimen.

Figure 5 Typical load-time curves - Series III.

Figure 6 Loading program for tests of Series II and III.

Figure 7 Variation of yield stress with hydrostatic pressure.

Figure 8 Intersection of initial and subsequent yield surface with $p - \sigma_1$ plane.

Figure 9 Bulge formation due to loading path OCD.